ISLETS
2022, VOL. 14, NO. 1, 1–13
https://doi.org/10.1080/19382014.2021.1982325

Identification of protease serine S1 family member 53 as a mitochondrial protein in murine islet beta cells

Noriko Mizusawa[a*], Nagakatsu Harada[b*], Takeo Iwata[c], Izumi Ohigashi[d], Mitsuo Itakura[e], and Katsuhiko Yoshimoto[a]

[a]Department of Medical Pharmacology, Institute of Biomedical Sciences, Tokushima University, Tokushima, Japan; [b]Department of Health and Nutrition, Faculty of Nursing and Nutrition, The University of Shimane, Shimane, Japan; [c]Department of Functional Morphology, Faculty of Pharmaceutical Sciences, Niigata University of Pharmacy and Applied Life Sciences, Niigata, Japan; [d]Division of Experimental Immunology, Institute of Advanced Medical Sciences, Tokushima University, Tokushima, Japan; [e]Division of Genetic Information, Institute for Genome Research, Tokushima University, Tokushima, Japan

ABSTRACT

The aim of this study was to identify genes that are specifically expressed in pancreatic islet β-cells (hereafter referred to as β-cells). Large-scale complementary DNA-sequencing analysis was performed for 3,429 expressed sequence tags derived from murine MIN6 β-cells, through homology comparisons using the GenBank database. Three individual ESTs were found to code for protease serine S1 family member 53 (*Prss53*). *Prss53* mRNA is processed into both a short and long form, which encode 482 and 552 amino acids, respectively. Transient overexpression of myc-tagged Prss53 in COS-7 cells showed that Prss53 was strongly associated with the luminal surfaces of organellar membranes and that it underwent signal peptide cleavage and N-glycosylation. Immunoelectron microscopy and western blotting revealed that Prss53 localized to mitochondria in MIN6 cells. Short hairpin RNA-mediated *Prss53* knockdown resulted in *Ppargc1a* downregulation and *Ucp2* and *Glut2* upregulation. JC-1 staining revealed that the mitochondria were depolarized in *Prss53*-knockdown MIN6 cells; however, no change was observed in glucose-stimulated insulin secretion. Our results suggest that mitochondrial Prss53 expression plays an important role in maintaining the health of β-cells.

ARTICLE HISTORY
Received 14 May 2021
Revised 12 September 2021
Accepted 13 September 2021

KEYWORDS
Prss53; pancreatic β-cell; MIN6; mitochondria

Introduction

Pancreatic islet β-cells (hereafter referred to as β-cells) are highly differentiated cells with cell-specific gene functions that contribute to physiological homeostasis in the body.[1] Besides the genes encoding insulin, amylin, or PDX-1, several genes have been recently reported to be expressed predominantly or preferentially in pancreatic islets or β-cells.[2–5] However, most genes responsible for the molecular basis of β-cell functions remain unidentified. We generated a complementary DNA (cDNA) library and determined the expression profile of MIN6 cells, one of the best-studied β-cell lines.[6,7] In general, gene-expression differences have been determined using oligonucleotide microarrays to detect mRNA levels in cells[8] or tissues,[9] or under several pathological or physiological conditions, such as normal cells versus tumor cells,[10] caloric restriction,[11] or cells exposed to various glucose concentrations.[12] Moreover, large-scale cDNA-sequencing analysis is advantageous for generating a catalog of expressed genes in target cells or tissues,[13,14] and a pool of unknown expressed sequence tags (ESTs) obtained from such profiling would provide a source of novel genes.[15,16]

Expression profiling in target cells or tissues of interest, based on the GenBank database, is useful for predicting target-specific gene expression, which can be experimentally confirmed. The primary purpose of this study was to discover novel β-cell-specific genes. We sequenced 3429 EST clones derived from a MIN6 cDNA library and

CONTACT Noriko Mizusawa mizusawa@tokushima-u.ac.jp Department of Oral Bioscience, Institute of Biomedical Sciences, Tokushima University Graduate School, 3-Kuramoto-cho, Tokushima City 770-8504, Japan

*These authors contributed equally to this work.

This article has been corrected with minor changes. These changes do not impact the academic content of the article.

Supplemental data for this article can be accessed on the publisher's website.

categorized them against the EST database (dbEST). Consistent with the *in-silico* predictions for β-cell-specific ESTs, expression of the protease serine S1 family member 53 (*Prss53*) gene was confirmed to be limited to MIN6 cells or pancreatic islets.

Results

Identification of Prss53 using EST analysis

Random sequencing yielded 3492 clones, among which 438 (12.8%) were poorly characterized *in silico*. For these 438 clones, the dbEST contained 13 EST entries from pancreatic islet libraries. Of these, nine ESTs were derived from more than four tissue libraries, whereas the remaining four ESTs were derived from only two or three tissue libraries, including pancreatic islet libraries. Among the four ESTs, three clones encoded overlapping sequences of the *Prss53* gene (Figure 1(a)). Northern blotting and quantitative reverse transcription polymerase chain reaction (qRT-PCR) analyses revealed that *Prss53* was expressed specifically in MIN6 cells and pancreatic islets (Figure 1(b,c)). Additionally, *Prss53* expression was downregulated in obese and diabetic KK-Ay mice, when compared with KK mice (Figure 1(d)).

Characterization of Prss53 isoforms

The estimated molecular masses of the short isoform (482 amino acids) and long isoform (552 amino acids) of Prss53 were 51.5 and 59.0 kDa, respectively (Figure 1(e), S1C). Alignment of the long Prss53 isoform with other known proteins revealed the presence of repeated catalytic triad (His, Asp, and Ser) motifs, which are observed in serine proteases (Figures S1C and S2C). This long Prss53 isoform contained nine conserved Cys residue repeats (Figure S2C). The short Prss53 isoform lacked exon 10, which encodes the second Ser residue in the active site. RT-PCR analysis using

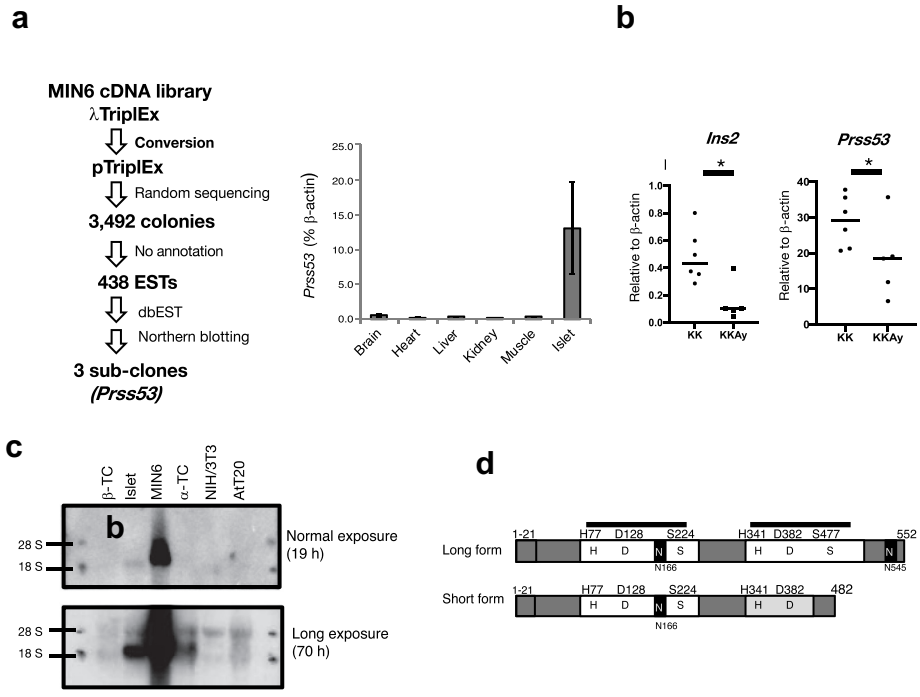

Figure 1. Detection of upregulated *Prss53* expression in MIN6 cells. a. Scheme for detecting *Prss53* upregulation using random cDNA sequencing. Of the 3429 clones identified *in silico*, we focused on three common *Prss53*-encoding clones. **b**. Northern blotting analysis of *Prss53* expression in MIN6 cells and mouse pancreatic islets. 28S and 18S ribosomal RNAs were approximately 5 kb and 2 kb in size. **c**. qRT-PCR analysis of C57BL/6 J mouse tissues. **d**. *Prss53* expression in islets obtained from KK and KK-Ay mice. Data were plotted using GraphPad Prism software. **e**. Schematic illustration of murine Prss53 isoforms, comprised of 482 or 552 amino acids. Repeated triads, characteristic of serine proteases (the first unit: His^{77}, Asp^{128}, and Ser^{224}; the second unit: His^{341}, Asp^{382}, and Ser^{477}). N-glycosylation were observed at N^{166} and N^{545}. A hydrophobic region is represented within the black box at the NH_2-terminus.

primers that target full-length *Prss53* revealed a short isoform (1730 bp) and a long isoform (1947 bp): the expression level of the long isoform was higher than that of the short isoform (Figure S1A).

Typical consensus sites for N-glycosylation, i.e., the Asn-X-(Thr/Ser) motif, were detected at N^{166} and N^{545} in the long Prss53 isoform, whereas only one N-glycosylation site (N^{166}) was detected in the short Prss53 isoform. Signal P (http://www.cbs.dtu.dk/services/SignalP/), a program developed by Nielsen et al.,[21] was used to predict the presence of a cleavage site for the signal peptide between Ala (A)[17] and Ala (A)[18] for mouse Prss53, or Gly (G)[19] and Gln (Q)[20] for human Prss53 (Figure S2B). the presence of a cleavage site for the signal peptide between Ala (A)[17] and Ala (A)[18] for mouse Prss53, or Gly (G)[19] and Gln (Q)[20] for human Prss53 (Figure S2B).

Exogeneous Prss53-expression analysis

A myc-tagged variant of Prss53 was confirmed to have a higher molecular weight than wild-type (non-tagged) Prss53 (Figure 2(a)). After transfecting COS-7 cells with the myc-Prss53 expression plasmid, both the short and long isoforms of Prss53 were only detected in cell extracts and not in the culture medium, indicating that Prss53 was not secreted (Figure 2(b)). Further, Prss53-expressing COS-7 cells were incubated with tunicamycin (Tunica; an inhibitor of N-glycosylation) or phenyl-N-acetyl-α-

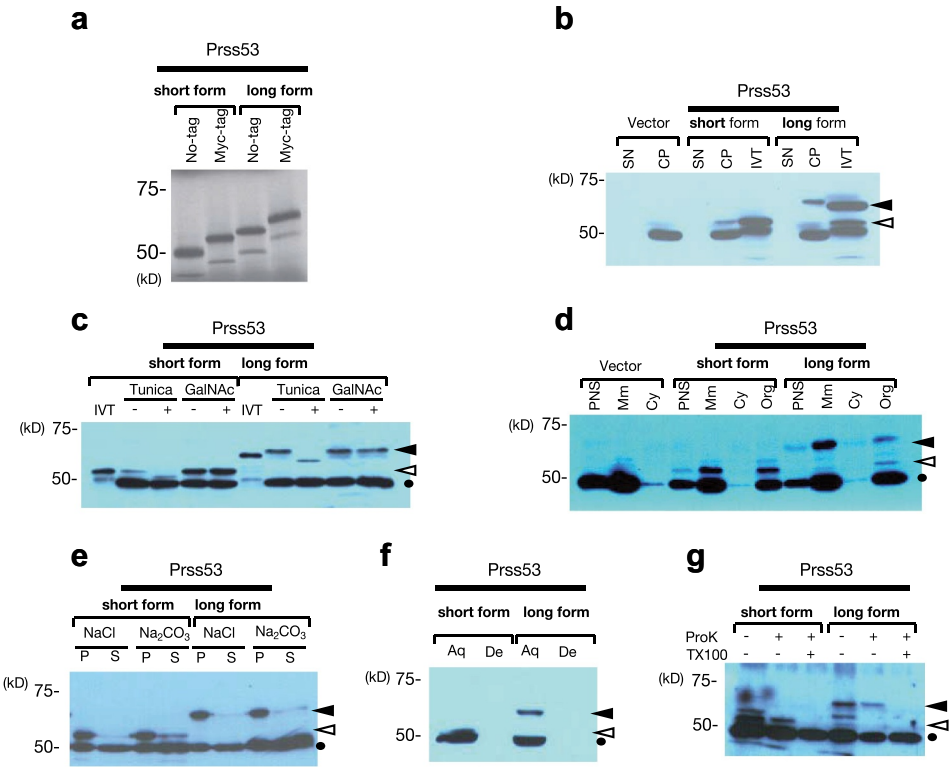

Figure 2. Characterization of Prss53 expression in COS7 cells. a. Molecular sizes of *in vitro*-translated Prss53 in the presence of ^{20S} methionine. Both the short (51.5 kDa) and long (59.0 kDa) isoforms of Prss53 were synthesized with (myc-tag) or without (No tag) a myc-epitope tag. **b**. Myc-tagged Prss53 expression was examined in COS7 cell protein extract (CP) or culture supernatant medium (SN). IVT Prss53 was loaded as a size marker. **c**. Prss53-expressed-COS7 cells with tunicamycin (Tunica) or phenyl-N-acetyl-α-D-galactosaminide (GalNac). IVT Prss53 was loaded as a size marker. **d**. Subcellular fractionation of Prss53-expressing COS7 cells. PNS; post-nuclear supernatant, Mm; plasma membrane fraction, Cy; cytosolic fraction, Org; organellar fraction. **e**. The pellet (P) and supernatant (S) of the Org fraction were resuspended in a homogenizing buffer without Triton X-100 and diluted 50–100-fold in 1 M NaCl or 100 mM Na_2CO_3, after which they were incubated on ice or 30 min. **f**. After mixing the Org fraction with Triton X-114, it was separated into an aqueous layer (Aq) and a detergent layer (De). **g**. Protease K-protection assay. The Org fraction was incubated with or without proteinase K (Pro K), in the presence of absence of Triton X-100 (TX100). The open and closed arrowheads indicate the short and long isoforms of Prss53, respectively. Nonspecific bands were observed at 50 kDa. The results of western blotting analysis with an anti-myc tag antibody are shown.

D-galactosaminide (GalNAc; an inhibitor of mucin-like O-glycosylation). Only tunicamycin treatment decreased the size of both the short and long isoforms of Prss53 (Figure 2(c)). Furthermore, proteins treated with tunicamycin were smaller than those translated *in vitro*. The decreased molecular weights of the Prss53 isoforms in COS-7 cells after tunicamycin treatment, compared to those of Prss53 translated *in vitro* (Figure 2(c)), suggests that the signal peptide (amino acids 1–23; calculated molecular weight = 2.5 kDa) was cleaved during co-translation. The two N-glycosylation sites (N166 and N545, molecular weight of each N-glycosylation group = 2–3 kDa; Figure 1(e)) for the Prss53 long form, after release of the signal peptide (2.5 kDa) in COS-7 cells, might account for the larger molecular weight (the net result is an increase of about 2.5 kDa) of this protein compared to the *in vitro*-translated (IVT) proteins (Figure 2(b)). In contrast, preventing N-glycosylation at one site (N166) in the short Prss53 isoform, whose signal peptide (2.5 kDa) is released in cells, made its size apparently the same as that synthesized *in vitro* (Figure 2(b)). Centrifugally fractionated lysates from myc-*Prss53*-expressing COS-7 cells were used to analyze the interaction of Prss53 with organellar (Org) membranes. The Org fraction mainly comprised organellar membranes from the rough and smooth endoplasmic reticulum, Golgi apparatus, and mitochondria.

Association of Prss53 with organellar membranes

The Org fraction of myc-*Prss53*-expressing COS-7 cells was treated with Na_2CO_3, which disrupts vesicles, resulting in the release of soluble or peripheral proteins, where the membrane proteins remained bound to the membrane. Prss53 was detected in the pellet fraction after extraction with sodium chloride (control) or Na_2CO_3 (Figure 2(e)), indicating that Prss53 is a peripheral protein associated with organellar membranes. Next, the transmembrane-spanning region of Prss53 was examined using a phase-separation method with Triton X-114. myc-tagged Prss53 partitioned completely into the aqueous supernatant, indicating that Prss53 was not expressed as a transmembrane protein, despite the prediction made by the TMpred program (Figure 2(f)). Furthermore, the location of Prss53 (inside or outside the membrane) was examined by performing proteinase K-protection assays. In the absence of Triton X-100, proteinase K did not digest myc-tagged Prss53. However, treatment with Triton X-100 promoted proteinase K-mediated digestion of myc-tagged Prss53 (Figure 2(f)), indicating that Prss53 was bound to the membrane. Thus, Prss53 is a peripheral protein associated with the luminal surface that is not integrated into the membrane and is associated with some organelles.

Mitochondrial localization of the Prss53 protein

Prss53 expression was detected in insulin-positive cells (Figure 3(a,b)) from mouse pancreatic tissues. Transmission electron microscopy analysis of MIN6 cells revealed that Prss53 was localized to mitochondria (Figure 3(c)). Western blotting analysis revealed that Prss53 separated into the mitochondrial fraction of MIN6 cells (Figure 3(d)).

Effect of Prss53 knockdown in MIN6 cells

Lentiviral short-hairpin RNA (shRNA)-mediated *Prss53* knockdown was performed in MIN6 cells to examine the function of Prss53. When testing different shRNAs against the *Prss53* gene, the most effective shRNA was found to be #KD1 (Figures S3). *Prss53* knockdown did not affect the expression levels of various genes, including *Ins2* (an insulin-coding gene) and *Pdx1*. Decreased *Ppargc1a*/Pgc1α expression and increased *Ucp2* and *Glut2* expression occurred after *Prss53* knockdown in MIN6 cells (Figure 4(a,b)). These results suggest that mitochondrial dysfunction occurred in *Prss53*-knockdown MIN6 cells. Staining with the dye, 5,5′,6,6′-tetrachloro-1,1′,3,3′-tetraethyl benzimidazole carbocyanine iodide (JC-1), an indicator used to study mitochondrial-membrane potentials, revealed that mitochondrial depolarization decreased in *Prss53*-knockdown MIN6 cells (Figure 4(c,d)), suggesting that the health of the cells became poor following Prss53 knockdown. However, glucose-stimulated insulin secretion (GSIS) was not affected in these cells (Figure 4(e)).

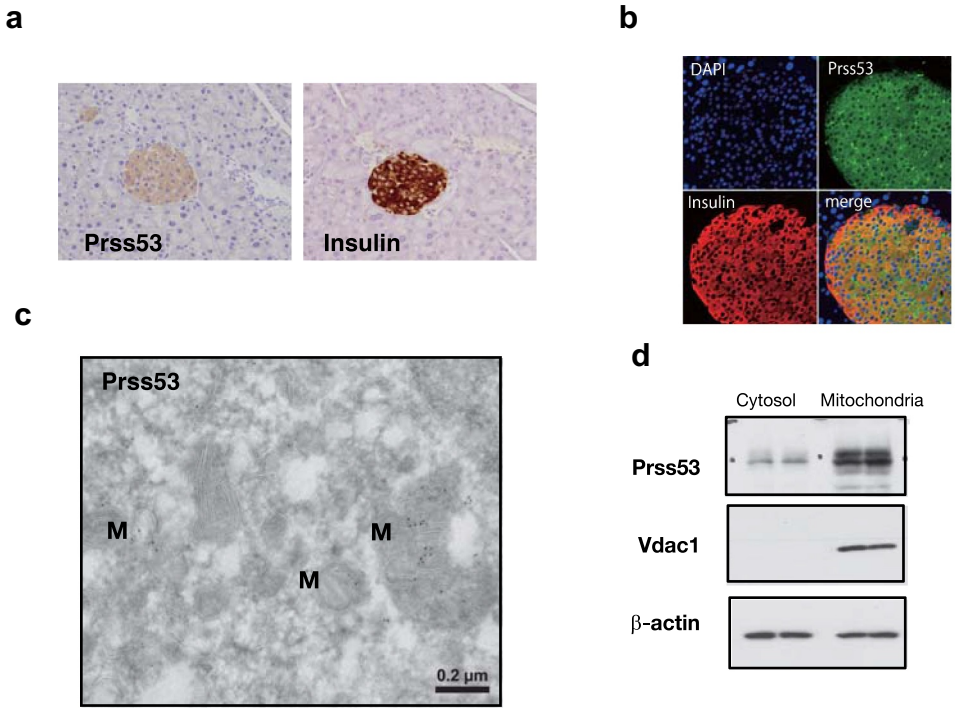

Figure 3. Mitochondrial localization of Prss53 in MIN6 cells. a. Representative immunostaining images of Prss53 and insulin in tissues from C57BL/6 mice. **b**. Overlapping fluorescence images of Prss53 (green) and insulin (red), a marker of pancreatic β-cells. **c**. Transmission-immunoelectron micrographs. Localization to mitochondria (M) was determined based on the localization of gold particles. **d**. Subcellular fractionation for subsequent western blotting analysis with antibodies against Prss53, Vdac1 (a mitochondrial marker), and Actb (a cytosolic marker).

Discussion

In this study, we identified a prominently expressed gene (*Prss53*) in MIN6 cells and murine islets. *Prss53* was not annotated before this study was started. In 2006, Santiago et al. reported a unique protein with tandem serine-protease domains within the same polypeptide chain, which was named POLYSERASE-3.[23] Waanders et al. performed direct proteomic analysis of single pancreatic islets and demonstrated the expression of the hypothetical POLYSERASE-3 protein in mice.[24] Furthermore, because the amino acid sequences around these active sites have been confirmed to be moderately similar to those of clan A, the S1 family of serine proteases,[25] POLYSERASE-3 was also termed PRSS53. Tonne et al. demonstrated that *Prss53* was expressed in wild-type islets and that *Prss53* expression was downregulated in a mouse model of streptozotocin-induced type-1 diabetes (T1D), indicating that Prss53 may serve a role in β-cell function.[26] We showed that *Prss53* expression was downregulated in KK-Ay mice (Figure 1(d)), which have been used to model T2D and obesity. These results suggest that correlations exist between Prss53-expression levels and the etiologies of acute T1D and chronic T2D.

Prss53 expression (at least that of the long form) was detected in the mitochondria of murine β-cells. Because Prss53 shares high homology with other serine proteases, few sites could be selected as candidate epitope sequences for producing a polyclonal antibody (Figure S2C). Hence, the custom generated anti-Prss53 antibody only detected the long form of Prss53. The shRNA-mediated knockdown of *Prss53* resulted in mitochondrial dysfunction as evidenced by changes in the fluorescence of the JC-1 dye, a mitochondrial indicator, and gene expression differences (Figure 4(c,d)). *Prss53* knockdown did not affect *Ins2* expression or that of its transcription factor *Pdx1*, an essential protein for β-cells.[17,27] In contrast, *Prss53* knockdown downregulated *Ppargc1a*/Pgc1α expression and upregulated *Ucp2 and Glut2* expression (Figure 4(a,b)). *Ppargc1a*/Pgc1α is a transcriptional co-activator that interacts

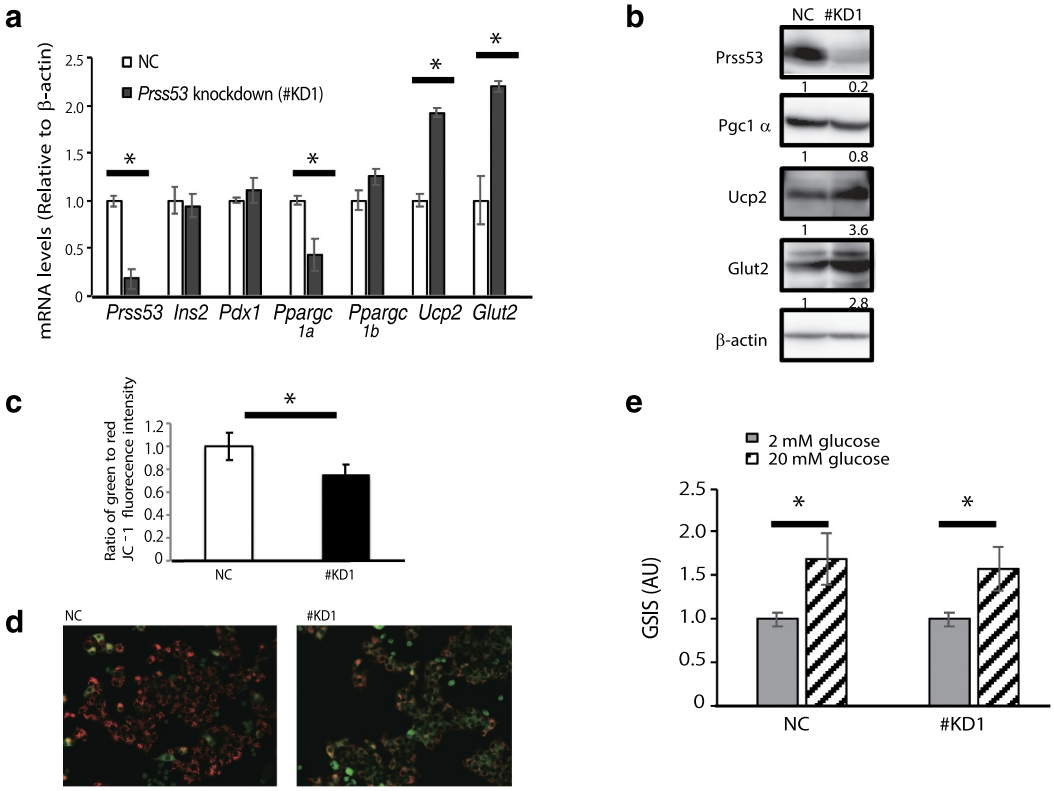

Figure 4. Effect of *Prss53* knockdown on MIN6 cells. a. Cells were transduced with a lentivirus to knock down *Prss53* expression. qRT-PCR analysis revealed that *Prss53* expression was successfully knocked down in MIN6 cells (#KD1), compared with that in the negative control (NC) cells (n = 4). **b**. Western blot analysis was performed using ImageJ software.[22] The numbers shown represent the signal intensities of the target proteins, normalized to that of β-actin. **c**. Mitochondrial-membrane potential assessments with JC-1 staining. Red: green ratios were calculated using a microplate reader. **d**. Fluorescence images with taken after JC-1 dye staining were obtained by fluorescence microscopy. **e**. GSIS in MIN6 cells. Values are shown as fold-changes relative to control conditions. AU, arbitrary units. *$P < .05$ versus NC.

with various transcription factors to regulate fatty acid metabolism, mitochondrial proteins, and antioxidant defense responses.[18,28] Nuclear respiratory factor 1 (NFR1) is coactivated by PGC1α, which in turns activates mRNA expression of the transcription factor A, mitochondrial (*TFAM*) gene, thus inducing mitochondrial DNA (mtDNA) synthesis.[29] The expression levels of PGC1α and NFR1 were significantly reduced in old animals, indicating that mitochondrial biogenesis was impaired.[30] TFAM is a protein that maintains the integrity of mtDNA, and alterations in TFAM expression have been associated with mitochondrial damage.[31] *Ppargc1a*/Pgc1α and *Nrf1* expression decreased in *Prss53*-knockdown MIN6 cells, although no direct transcriptional decrease in *Tfam* expression was observed (Figure 4(a) and S3D). *Pgc1α* expression was downregulated in the islets of patients with T2D and correlated with decreased insulin secretion,[19] and glucocorticoid-mediated *Pgc1α* overexpression in the fetal stage impairs adult β-cell function by downregulating *Pdx-1* expression.[27] These findings indicate that the functions of Pgc1*α* and its homolog Pgc1β in islets are not fully understood. In this study, knocking down *Prss53* expression slightly upregulated *Ppargc1β*/*Pgc1β* expression in MIN6 cells (Figure 4(a) and S3C). Thus, Pgc1β might serve a compensatory role in MIN6 cells. Glucose triggers insulin secretion by being metabolized to ATP within the β-cells. MtDNA depletion in β-cells has been shown to impair the GSIS response, emphasizing a critical role for mitochondria in insulin secretion.[20,32–34] Alterations in biochemical pathways that link glucose uptake with ATP generation could thus alter the GSIS response. Loss of GLUT2, a major glucose transporter in rodent islet β-cells,[35] reduces glucose uptake and ATP production.[20] Furthermore, Glut2

downregulation inhibits GSIS in genetic- and chemical-induced diabetes and in transplanted islets exposed to chronic hyperglycemia.[36] On the other hand, UCP2 is another mitochondrial protein that inhibits insulin secretion from β-cells.[37–39] The upregulation of Glut2 by Prss53 knockdown may provide a compensatory mechanism that enables normal insulin secretion, even in the presence of mitochondrial defects with elevated Ucp2. Dysregulated insulin secretion by β-cells and/or lowered insulin clearance by the liver results in chronically elevated insulin levels without hypoglycemia in individuals with obesity and metabolic disorders.[40,41] Further studies are needed to clarify the roles of PRSS53 in β-cells.

The murine Prss53 amino acid sequences exhibited 81.0% and 94.8% homology with human and rat PRSS53, respectively (Figure S2B). The high degrees of conservation among these species indicate the biological importance of PRSS53. In humans, PRSS53 expression is upregulated in hair follicles, especially in the inner root sheath. The Q30R substitution in PRSS53 affects enzyme processing and secretion.[42] Genes in the associated region of the single-nucleotide polymorphism rs10782001 may be responsible for the associated signaling.[43] This region includes *POL3S* (later as *PRSS53*), which was strongly associated with psoriatic arthritis (PsA). Patients with PsA are seronegative for rheumatoid factors. Psoriasis was previously reported to be associated with obesity and T2D.[44] A meta-analysis of observational studies indicated that the risk for developing T2D in patients with psoriasis and PsA was 1.76-fold higher than that in healthy individuals.[45] Another meta-analysis of 22 critically evaluated observational studies revealed that the risk of developing T2D in patients with psoriasis was 1.42-fold higher than that in healthy controls.[46] Interestingly, *PRSS53* expression has only been reported in the skin and has been correlated with inflammation in humans. Tissue-specific expression of *PRSS53* may vary with species.

Mitochondria are involved in energy production and in various and diverse signaling pathways. The elucidation of PRSS53 functions might open the possibility of developing new therapies for diabetes and mitochondria-related diseases. Further studies are needed to clarify the roles of PRSS53 in relation to mitochondrial functions.

Materials and methods

Cells and animals

MIN6 cells were cultured in Dulbecco's Modified Eagle Medium (DMEM) (Wako; 044–29765) supplemented with 25 mM glucose and 10% fetal bovine serum (FBS). αTC1.6, βTC1.6, NIH3T3, AtT20, and COS7 cells were cultured in DMEM supplemented with 5.5 mM glucose and 10% FBS. C57BL/6 J, KK, and KK-Ay mice were obtained from Clea Japan, Inc. The animal studies were approved by the Institutional Animal Care and Use Committee of Tokushima University (approval number 05323). To isolate murine islets, 0.25 mg/mL of liberase RI (Roche; 05401020001) was injected into the pancreatic duct. Each isolated pancreas was digested at 37°C for 40 min. The tissues were washed, and the islets were hand-picked. Total RNA was extracted from the freshly isolated islets of 10-week-old mice and subjected to qRT-PCR analysis.

Construction of a cDNA library from MIN6 cells

Total RNA was isolated from cultured MIN6 cells using ISOGEN (Nippon Gene). A cDNA library of the MIN6 cells was constructed using the λTriplEx phage vector (Clontech). Briefly, first-strand cDNA was synthesized with oligo (dT) primers (5′-GTCGACTCTAGATTTTTTTTTTTTTTT-3′) containing an *XbaI* site (underlined). The cDNAs with a length of >400 base pairs (bp) were cloned into the *Eco*RI and *Xba*I sites of the λTriplEx phage vector. The *Eco*RI and *Xba*I sites of the λTriplEx vector were flanked by two *loxP* sites, and MIN6 cDNA were introduced between the *loxP* sites. Transducing the *Escherichia coli* strain BM25.8 with λTriplEx lysate resulted in the release and circularization of pTriplEx, which was catalyzed by BM25.8-derived *Cre* recombinase. Colonies of the recombinant BM25.8 strain were selected for on culture plates containing ampicillin (50 μg/mL).

Large-scale cDNA sequencing

Individual pTriplEx clones were randomly selected and sequenced using a Big Dye Terminator Cycle Sequencing Kit (Applied Biosystems) for cDNA screening. Homologies between the sequences in the 5′-end (400–500 bp) and the nucleotide sequences of known genes and ESTs were examined using the BLASTN program of the National Center for Biotechnology Information (http://www.ncbi.nlm.nih. gov/).

Northern blotting analysis

Total RNA (20 μg) was subjected to denaturing agarose electrophoresis using a 1% agarose gel and transferred to a GeneScreen membrane with a pore size of 0.45 μm (NEN Life Science Products). Each insert in the pTriplEx vector (*Eco*RI–*Xba*I fragment) was labeled with [α-^{33}P] dCTP using a Megaprime labeling system (GE Healthcare Life Sciences) and used as a probe. The membrane was hybridized overnight with the probe at 42°C, washed, and exposed to Kodak BIOMAX^{TM} MS film at −80°C.

qRT-PCR analysis

Total RNA (500 ng) was subjected to reverse transcription using the PrimeScript RT-PCR Kit (Takara) and Thunderbird SYBR qPCR Mix (Toyobo). Quantitative real-time PCR (qPCR) was performed on an ABI PRISM 7300 instrument (Applied Biosystems Japan). The qPCR conditions were as follows: 95°C for 2 min, followed by 40 cycles of 95°C for 15 s and 60°C for 31 s. Relative quantification was performed by interpolating crossing point data on an independent standard curve, thereby accounting for any differences in amplification efficiency. The sequences of the primers used to amplify *Prss53*, and related target genes are shown in Figure S1 and Supplemental Table 1. *Actb* expression was detected as an internal standard.

Western blotting

The cells were washed with ice-cold phosphate-buffered saline (PBS) and incubated in a buffer (20 mM Tris-HCl [pH 7.4], 150 mM NaCl, 1% sodium deoxycholate, 0.1% sodium dodecyl sulfate [SDS], 1% Nonidet-P40, 2 mM ethylenediaminetetraacetic acid [EDTA], 10 μg/mL leupeptin, and 1 mM phenylmethyl sulfonyl fluoride [PMSF]) for 30 min on ice. The lysates were passed through a 21-gauge needle and centrifuged at 4°C and 13,500 × *g* for 30 min. Each supernatant was used as a cell lysate. Proteins from the culture medium were precipitated with cold acetone and resuspended in PBS. SDS-polyacrylamide gel electrophoresis (SDS-PAGE) was performed with 20 μg protein following blotting onto an Immobilon-P membrane with a pore size of 0.45 μm (Millipore). After blocking with Tris-buffered saline containing 5% milk and 0.05% Tween 20 for 1 h, the membranes were incubated with a primary anti-myc tag antibody (1:1000; New England Biolabs), followed by incubation with a horseradish peroxidase (HRP)-conjugated anti-rabbit immunoglobulin G (IgG) secondary antibody (1:2000; GE Healthcare). Immunoreactive bands were visualized using an Enhanced Chemiluminescence Plus Detection Kit (GE Healthcare), according to the manufacturer's instructions.

Cell-free transcription and translation

Prss53 protein was synthesized *in vitro* under the control of the T7 promoter using a transcription–translation coupled reticulocyte lysate system (Promega; L4611) with pCR-Blunt II-*Prss53* cDNA (including a stop codon) or pcDNA3.1/myc-His-*Prss53* cDNA at 30°C for 60–90 min in the presence of ^{20S} methionine, following the manufacturer's instructions.

Analysis of glycosylation

COS-7 cells were transfected for 24 h with the pcDNA3.1/myc-His-*Prss53* vector, using the PolyFect transfection reagent (Qiagen). The growth medium was replaced with serum-free medium, and the cells were cultured for an additional 24 h. The Prss53-expressing COS-7 cells were incubated for 24 h with the N-glycosylation inhibitor, tunicamycin (2.5 μg/mL; Sigma) or the mucin-like O-glycosylation inhibitor, phenyl-N-GalNac (2 mM; Sigma). Subsequently, total proteins were extracted from the cells, as described previously.[47]

Subcellular fractionation

pcDNA3.1/myc-His-*Prss53*-expressing COS-7 cells were washed thrice with PBS and scraped into a homogenizing buffer (10 mM Tris-HCl [pH 7.4], 0.25 M sucrose, 2 mM EDTA, and 1 mM PMSF). Next, the cells were homogenized using a Dounce homogenizer with 12 strokes of an A-type pestle. The homogenate was centrifuged at 1000 × *g* for 10 min to remove the nuclei and large cell fragments. The post-nuclear supernatant (PNS) was subjected to centrifugation at 105,000 × *g* for 60 min to obtain a membrane fraction (pellet; Mm) and a cytosolic fraction (supernatant; Cy). Additionally, the PNS was centrifuged at 10,000 × *g* for 12 min. The resulting supernatant was centrifuged at 105,000 × *g* for 60 min to obtain the Org fraction as a pellet. The Mm and Org fractions were resuspended in a homogenizing buffer containing 0.5% Triton X-100, and the homogenate was subjected to western blotting analysis. The Org fraction was used for further analysis.

Carbonate extraction

The Org fraction was resuspended in a homogenizing buffer (without Triton X-100), diluted 50–100-fold with 1 M NaCl or 100 mM Na_2CO_3 (pH 11.5), and incubated for 30 min on ice.[48] The suspension was centrifuged at 105,000 × *g* and 4°C for 60 min. The supernatant was concentrated to a volume of 5 µL using an Ultrafree-0.5 centrifugal filter (Millipore) at 12,000 × *g* for 40 min. The pellets were gently rinsed once with ice-cold water. The samples were resuspended in an SDS-containing sample buffer.

Protease-protection assay

The volume of the Org fraction (7 µL) was brought up to 11 µL in a buffer containing 50 mM Tris-HCl (pH 7.4), 100 mM NaCl, and 0.25 M sucrose. The sample was incubated on ice in the presence or absence of proteinase K (100 µg/mL) for 60 min. For pretreatment, Triton X-100 was added (final concentration of 1%) before adding proteinase K. The samples were directly mixed with SDS sample buffer.

Phase separation in Triton X-114

The phase-separation method used in this study was described previously.[49,5051] Briefly, the Org fraction was incubated in 100 µL of buffer (10 mM Tris-HCl [pH 7.4], 150 mM NaCl, and 1% Triton X-114) at 0°C for 15 min. The insoluble material was removed by centrifugation at 3000 × *g* for 5 min. The supernatant was layered onto 150 µL of a mixture comprising a sucrose cushion (6%), 10 mM Tris-HCl (pH 7.4), 150 mM NaCl, and 0.06% Triton X-114. The sample was incubated at 30°C for 5 min and centrifuged at 1000 × *g* and room temperature (approximately 22°C) for 3 min.

Immunohistochemical and immunofluorescence analyses

A customized rabbit polyclonal anti-Prss53 antibody was synthesized by Immuno-Biological Laboratories Co., using a VYFAEEPEPEAETGSC peptide. The murine pancreas was fixed in 4% paraformaldehyde (PFA), embedded in paraffin, permeabilized with methanol containing 0.3% hydrogen peroxide for 10 min, and incubated with the anti-Prss53 antibody and an anti-goat IgG antibody (1:200; negative control; Santa Cruz Biotechnology) at 37°C for 2 h. Next, the samples were incubated with Histofine Simple Stain MAX PO (Multi) or Histofine Simple Stain MAX PO (G) (Nichirei Co.) for 30 min, followed by incubation with the chromogen, 3, 3′-diaminobenzidine for 15 min. The nuclei were counterstained with Mayer's hematoxylin. For immunofluorescence analysis, the permeabilized sections were incubated with anti-Prss53 (rabbit IgG, 1:50) or anti-insulin (guinea pig IgG; 1:50) antibodies from Sigma. The sections were subsequently incubated with a mixture of Alexa Fluor 488-labeled anti-rabbit IgG donkey serum and Alexa Fluor 546-labeled anti-guinea pig IgG donkey serum (1:200; Molecular Probes, Inc.) at 37°C for 1.5 h. The sections were observed under a laser-scanning confocal microscope (LSM510; Zeiss). Negative-control samples were incubated with nonimmune normal sera, instead of primary antibodies.

Immunoelectron microscopy

MIN6 cell pellets were fixed in PBS containing 4% PFA for 30 min at 4°C and then incubated in PBS containing 30% sucrose solution for 30 min at room temperature. Next, the cells were transferred to 20% polyvinylpyrrolidone and rapidly frozen in Reichert KF-80 using liquid propane (−80°C), which was cooled with liquid nitrogen. The specimens were trimmed at −70°C, and frozen ultrathin sections were prepared using an ultramicrotome (Leica EM UC6/FC6, Leica) at −120°C.[52] The ultrathin sections were incubated with primary antibodies for 2 h. The samples were then incubated with antibodies conjugated with 5 nm gold particles (GE Healthcare) for 2 h. Electron micrographs were captured at 40 kV using a Hi-7100 electron microscope (Hitachi Co., Ltd.).

Isolation of mitochondria

Cytosolic and mitochondrial fractions were prepared using the Mitochondria Isolation Kit (Thermo Fisher Scientific), following the manufacturer's instructions. Western blotting was performed using an antibody against the mitochondrial marker Vdac1 (1:2000; Calbiochem).

Lentiviral-mediated knockdown of Prss53

Prss53 was knocked down in MIN6 cells using MISSON lentiviral transduction particles (SHCLNV-XM_284356, clone ID TRCN0000032807, TRC0000032804, TRC0000032805, and TRC00 00032806, designated here as #KD1, #KD2, #KD3, and #KD4, respectively; Sigma), following the manufacturer's protocol. Negative-control samples were transduced with an empty vector-containing virus (pLKO.1; catalog number, SHC016V; Sigma). The MIN6 cells were transduced at a multiplicity of infection of 10 in DMEM supplemented with 25 mM glucose, 10% FBS, and polybrene (8 mg/mL) for 18 h. Next, the cells were cultured in fresh medium. At 2 days post-transduction, the transduced MIN6 cells were selected by culturing them on a plate containing puromycin (800 ng/mL) for 2 weeks. For qRT-PCR analysis, the cells were seeded in 12-well plates and cultured for 48 h. For western blotting analysis, the cells were seeded in 60 mm plates and cultured for 24 – 48 h. Primary antibodies were diluted as indicated in Can Get Signal solution 1 (Toyobo): anti-Prss53 (1:2000), anti-Pgc1α (1:2000; Novus Biologicals), anti-Ucp2 (1:2;000; BioLegend), anti-Glut2 (1:2000; Novus biologicals) and anti-Actb (1:4000; Sigma). The samples were then incubated with HRP-conjugated rabbit anti-donkey IgG or anti-sheep mouse IgG (GE Healthcare) in Can Get Signal Solution 2.

JC-1 staining

Mitochondrial membrane potentials were assessed in MIN6 cells by performing JC-1-incorporation assays with the Mitochondrial Membrane Potential Assay Kit (Cayman Chemical), a microplate reader, and the JC-1 mitoMP Detection Kit (Dojindo) for fluorescence images. Healthy MIN6 cells were detected with a fluorometer using excitation and emission wavelengths of 560 and 595 nm (red), respectively, and dead cells were detected using excitation and emission wavelengths of 485 and 535 nm (green), respectively. The fluorescence ratio of free JC-1 monomers (green) to JC-1 aggregates in mitochondria (red) was measured with a fluorescence plate reader (Infinite 200 Pro, Tecan), and the fluorescence was observed using a BZ-X800 dual-emission fluorescence microscope (Keyence).

Measuring insulin concentrations

Insulin secretion into the culture medium from MIN6 cells was measured using the Mouse Insulin H-type™ Enzyme-Linked Immunosorbent Assay Kit (Shibayagi Co., Ltd.), according to the manufacturer's protocol. Briefly, MIN6 cells were cultured for 1 – 2 h in Krebs–Ringer bicarbonate (KRB) buffer (129 mM NaCl, 3.6 mM KCl, 0.5 mM NaH_2PO_4, 0.5 mM $MgSO_4$, 1.5 mM $CaCl_2$, 2 mM $NaHCO_3$, 10 mM HEPES, and 0.1% bovine serum albumin) containing 2.0 mM glucose. Next, the KRB buffer was changed to a buffer containing the indicated concentration of glucose (2.0 mM or 20 mM), and the cells were cultured for 1 h. The KRB buffer was collected and the insulin concentration was measured.

Statistical analysis

The data are represented as the mean ± standard deviation, where *n* represents the number of independent experiments. The means of different groups were compared using one-way analysis of variance. Differences were considered statistically significant at $P < .05$.

Acknowledgments

We thank Dr. J. Miyazaki for providing MIN6 cells, Dr. S. Hatakeyama for technical assistance with the microscopy experiments, Dr. H. Iwahana for his valuable comments, and *Editage* (www.editage.com) for English language editing. We obtained cooperation from many people in the Otsuka Department of Clinical and Molecular Nutrition Laboratory at Tokushima University. This work was supported by the Ministry of Education, Culture, Sports, Science and Technology of Japan through grants from Grants-in-Aid for Scientific Research [grant numbers JP15590943 and JP21K11698].

Disclosure statement

No potential conflict of interest was reported by the author(s).

Funding

This work was supported by the the Ministry of Education, Culture, Sports, Science and Technology of Japan [JP21K11698]; the Ministry of Education, Culture, Sports, Science and Technology of Japan [JP15590943].

ORCID

Noriko Mizusawa http://orcid.org/0000-0001-6432-5355

Data availability statement

The data that support the findings of this study are available from the corresponding author, N. Mizusawa, upon reasonable request.

References

1. Steiner DF, James DE. Cellular and molecular biology of the beta cell. Diabetologia. 1992;35(S2):S41–S48. doi:10.1007/BF00586278.
2. Wagner L, Oliyarnyk O, Gartner W, Nowotny P, Groeger M, Kaserer K, Waldhausl W, Pasternack MS. Cloning and expression of secretagogin, a novel neuroendocrine- and pancreatic islet of Langerhans-specific Ca^{2+}-binding protein. J Biol Chem. 2000;275(32):24740–24751. doi:10.1074/jbc.M001974200.
3. Serre-Beinier V, Le Gurun S, Belluardo N, Trovato-Salinaro A, Charollais A, Haefliger JA, Condorelli DF, Meda P. Cx36 preferentially connects beta-cells within pancreatic islets. Diabetes. 2000;49(5):727–734. doi:10.2337/diabetes.49.5.727.
4. Shiraishi A, Yamada Y, Tsuura Y, Fijimoto S, Tsukiyama K, Mukai E, Toyoda Y, Miwa I, Seino Y. A novel glucokinase regulator in pancreatic beta cells: precursor of propionyl-CoA carboxylase beta subunit interacts with glucokinase and augments its activity. J Biol Chem. 2001;276(4):2325–2328. doi:10.1074/jbc.C000530200.
5. Arden SD, Zahn T, Steegers S, Webb S, Bergman B, O'Brien RM, Hutton JC. Molecular cloning of a pancreatic islet-specific glucose-6-phosphatase catalytic subunit-related protein. Diabetes. 1999;48(3):531–542. doi:10.2337/diabetes.48.3.531.
6. Tanaka M, Katashima R, Murakami D, Adzuma K, Takahashi Y, Tomonari A, Iwahana H, Yoshimoto K, Itakura M. Molecular cloning of a group of mouse pancreatic islet beta-cell-related genes by random cDNA sequencing. Diabetologia. 1995;38(4):381–386. doi: 10.1007/BF00410274.
7. Miyazaki J, Araki K, Yamato E, Ikegami H, Asano T, Shibasaki Y, Oka Y, Yamamura K. Establishment of a pancreatic beta cell line that retains glucose-inducible insulin secretion: special reference to expression of glucose transporter isoforms. Endocrinology. 1990;127(1):126–132. doi:10.1210/endo-127-1-126.
8. Boeuf S, Klingenspor M, Van Hal NL, Schneider T, Keijer J, Klaus S. Differential gene expression in white and brown preadipocytes. Physiol Genomics. 2001;7(1):15–25. doi:10.1152/physiolgenomics.00048.2001.
9. Campbell WG, Gordon SE, Carlson CJ, Pattison JS, Hamilton MT, Booth FW. Differential global gene expression in red and white skeletal muscle. Am J Physiol Cell Physiol. 2001;280(4):C763–C768. doi:10.1152/ajpcell.2001.280.4.C763.
10. Graveel TJ, Jatkoe T, Madore SJ, Holt AL, Farnham PJ. Expression profiling and identification of novel genes in hepatocellular carcinomas. Oncogene. 2001;20(21):2704–2712. doi:10.1038/sj.onc.1204391.
11. Cao SX, Dhahbi JM, Mote PL, Spindler SR. Genomic profiling of short- and long-term caloric restriction effects in the liver of aging mice. Proc Natl Acad Sci U S A. 2001;98(19):10630–10635. doi:10.1073/pnas.191313598.
12. Webb GC, Akbar MS, Zhao C, Steiner DF. Expression profiling of pancreatic beta cells: glucose regulation of secretory and metabolic pathway genes. Proc Natl Acad Sci U S A. 2000;97(11):5773–5778. 2007. s135. doi:10.2337/diabetes.50.

13. Maeda K, Okubo K, Shimomura I, Mizuno K, Matsuzawa Y, Matsubara K. Analysis of an expression profile of genes in the human adipose tissue. Gene. 1997;190(2):227–235. doi:10.1016/s0378-1119(96)00730-5.
14. Hu RM, Han ZG, Song HD, Peng YD, Huang QH, Ren SX, Gu YJ, Huang CH, Li YB, Jiang CL, et al. Gene expression profiling in the human hypothalamus-pituitary-adrenal axis and full-length cDNA cloning. Proc Natl Acad Sci U S A. 2000;97(17):9543–9548. doi:10.1073/pnas.160270997.
15. Maeda K, Okubo K, Shimomura I, Funahashi T, Matsuzawa Y, Matsubara K. cDNA Cloning and expression of a novel adipose specific collagen-like factor, apM1 (adipose most abundant gene transcript). Biochem Biophys Res Commun. 1996;221(2):286–289. doi:10.1016/j.bbrc.2012.08.023.
16. Kok LD, Tsui SK, Waye M, Liew CC, Lee CY, Fung KP. Cloning and characterization of a cDNA encoding a novel fibroblast growth factor preferentially expressed in human heart. Biochem Biophys Res Commun. 1999;255(3):717–721. doi:10.1006/bbrc.1999.0178.17.
17. Jonsson J, Carlsson L, Edlund T, Edlund H. Insulin-promoter-factor 1 is required for pancreas development in mice. Nature. 1994;371(6498):606–609. doi:10.1038/371606a0.
18. St-Pierre J, Drori S, Uldry M, Silvaggi JM, Rhee J, Jäger S, Handschin C, Zheng K, Lin J, Yang W, et al. Suppression of reactive oxygen species and neurodegeneration by the PGC-1 transcriptional coactivators. Cell. 2006;127(2):397–408. doi:10.1016/j.cell.2006.09.024.
19. Ling C, Del Guerra S, Lupi R, Rönn T, Granhall C, Luthman H, Masiello P, Marchetti P, Groop L, Del Prato S. Epigenetic regulation of PPARGC1A in human type 2 diabetic islets and effect on insulin secretion. Diabetologia. 2008;51(4):615–622. doi:10.1007/s00125-007-0916-5.
20. Low BSJ, Lim CS, Ding SSL, Tan YS, Ng NHJ, Krishnan VG, Ang SF, Neo CWY, Verma CS, Hoon S, et al. Decreased GLUT2 and glucose uptake contribute to insulin secretion defects in MODY3/HNF1A hiPSC-derived mutant β cells. Nat Commun. 2021;12(1):3133. doi:10.1038/s41467-021-22843-4.
21. Nielsen H, Engelbrecht J, Brunak S, von Heijne G. Identification of prokaryotic and eukaryotic signal peptides and prediction of their cleavage sites. Protein Eng. 1997;10(1):1–6. doi:10.1093/protein/10.1.1.
22. Schneider CA, Rasband WS, Kw E. NIH Image to ImageJ: 25 years of image analysis. Nat Methods. 2012;9(7):671–675. doi:10.1038/nmeth.2089.
23. Cal S, Peinado JR, Llamazares M, Quesada V, Moncada-Pazos A, Garabaya C, López-Otín C. Identification and characterization of human polyserase-3, a novel protein with tandem serine-protease domains in the same polypeptide chain. BMC Biochem. 2006;7(1):9. doi:10.1186/1471-2091-7-9.
24. Waanders LF, Chwalek K, Monetti M, Kumar C, Lammert E, Mann M. Quantitative proteomic analysis of single pancreatic islets. Proc Natl Acad Sci U S A. 2009;106(45):18902–18907. doi:10.1073/pnas.0908351106.
25. Rawlings ND, Barrett AJ. Families of serine peptidases. Methods Enzymol. 1994;244:19–61. doi:10.1016/0076-6879(94)44004-2.
26. Tonne JM, Sakuma T, Deeds MC, Munoz-Gomez M, Barry MA, Kudva YC, Ikeda Y. Global gene expression profiling of pancreatic islets in mice during streptozotocin-induced beta-cell damage and pancreatic Glp-1 gene therapy. Dis Model Mech. 2013;6:1236–1245. doi:10.1242/dmm.012591.
27. Valtat B, Riveline J-P, Zhang P, Singh-Estivalet A, Armanet M, Venteclef N, Besseiche A, Kelly DP, Tronche F, Ferré P, et al. Fetal PGC-1 Overexpression Programs Adult Pancreatic -Cell Dysfunction. Diabetes. 2013;62(4):1206–1216. doi:10.2337/db12-0314.
28. Kaufman BA, Li C, Soleimanpour SA. Mitochondrial regulation of beta-cell function: maintaining the momentum for insulin release. Mol Aspects Med. 2015;42:91–104. doi:10.1016/j.mam.2015.01.004.
29. Puigserver P, Wu A, Park CW, Graves R, Wright M, Spiegelman BM. A cold-inducible coactivator of nuclear receptors linked to adaptive thermogenesis. Cell. 1998;92(6):829–839. doi:10.1016/S0092-8674(00)81410-5.
30. Viña J, Gomez-Cabrera MC, Borras C, Froio T, Sanchis-Gomar F, Martinez-Bello VE, Pallardo FV. Mitochondrial biogenesis in exercise and in ageing. Adv Drug Deliv Rev. 2009;61(14):1369–1374. doi:10.1016/j.addr.2009.06.006.
31. Franco DG, Moretti IF, Marie SKN. Mitochondria transcription factor A: a putative target for the effect of melatonin on U87MG malignant glioma cell line. Molecules. 2018;23(5):1129. doi:10.3390/molecules23051129.
32. Hayakawa T, Noda M, Yasuda K, Yorifuji H, Taniguchi S, Miwa I, Sakura H, Terauchi Y, Hayashi J-I, Sharpe GWG, et al. Ethidium Bromide-induced inhibition of mitochondrial gene transcription suppresses glucose-stimulated insulin release in the mouse pancreatic β-Cell line βHC9. J Biol Chem. 1998;273(32):20300–20307. doi:10.1074/jbc.273.32.20300.
33. McMillan RP, Stewart S, Budnick JA, Caswell CC, Hulver MW, Mukherjee K, Srivastava S. Quantitative variation in m.3243A > G mutation produce discrete changes in energy metabolism. 2019;9:5752. doi:10.1038/s41598-019-42262-2.
34. Henquin JC. Triggering and amplifying pathways of regulation of insulin secretion by glucose. Diabetes. 2000;49(11):1751–1760. doi:10.2337/diabetes.49.11.1751.

35. Takata K, Kasahara M, Oka Y, Hirano H. Mammalian Sugar Transporters:Their Localization and Link to Cellular Functions. ACTA HISTOCHEMICA ET CYTOCHEMICA. 1993;26(3):165–178. doi:10.1267/ahc.26.165.
36. Zangen DH, Bonner-Weir S, Lee CH, Latimer JB, Miller CP, Habener JF, Weir GC. Reduced insulin, GLUT2, and IDX-1 in -Cells after partial pancreatectomy. Diabetes. 1997;46(2):258–264. doi:10.2337/diab.46.2.258.
37. Li Y, Maedler K, Shu L, Haataja LUCP-2, Vella A. UCP-2 and UCP-3 proteins are differentially regulated in pancreatic Beta-Cells. PLoS One. 2008;3(1):e1397. doi:10.1371/journal.pone.0001397.
38. Robson-Doucette CA, Sultan S, Allister EM, Wikstrom JD, Koshkin V, Bhattacharjee A, Prentice KJ, Sereda SB, Shirihai OS, Wheeler MB. Beta-cell uncoupling protein 2 regulates reactive oxygen species production, which influences both insulin and glucagon secretion. Diabetes. 2011;60(11):2710–2719. doi:10.2337/db11-0132.
39. Zhang CY, Baffy G, Perret P, Krauss S, Peroni O, Grujic C, Hagen T, Vidal-Puig AJ, Boss O, Kim YB, et al. Uncoupling protein-2 negatively regulates insulin secretion and is a major link between obesity, β cell dysfunction, and type 2 diabetes. Cell. 2012;105(6):745–755. doi:10.1016/S0092-8674(01)00378-6.
40. Thomas DD, Corkey BE, Istfan NW, Apovian CM. Hyperinsulinemia: an early indicator of metabolic dysfunction. J Endocr Soc. 2019;3(9):1727–1747. doi:10.1210/js.2019-00065.
41. Kaga H, Tamura Y, Takeno K, Kakehi S, Funayama T, Furukawa Y, Nishitani-Yokoyama M, Shimada K, Daida H, Aoki S, et al. Correlates of insulin clearance in apparently healthy non-obese Japanese men. Sci Rep. 2017;7(1):1462. doi:10.1038/s41598-017-01469-x.
42. Adhikari K, Fontanil T, Cal S, Mendoza-Revilla J, Fuentes-Guajardo M, Chacon-Duque JC, Al-Saadi F, Johansson JA, Quinto-Sanchez M, Acuña-Alonzo V, et al. A genome-wide association scan in admixed Latin Americans identifies loci influencing facial and scalp hair features. Nat Commun. 2016;7(1):10815. doi:10.1038/ncomms10815.
43. Stuart PE, Nair RP, Ellinghaus E, Ding J, Tejasvi T, Gudjonsson JE, Li Y, Weidinger S, Eberlein B, Gieger C, et al. Genome-wide association analysis identifies three psoriasis susceptibility loci. Nat Genet. 2010;42(11):1000–1004. doi:10.1038/ng.693.
44. Lonnberg AS, Skov L, Skytthe A, Kyvik KO, Pedersen OB, Thomsen SF. Association of psoriasis with the risk for type 2 diabetes mellitus and obesity. JAMA Dermatol. 2016;152(7):761–767. doi:10.1001/jamadermatol.2015.6262.
45. Coto-Segura P, Eiris-Salvado N, González-Lara L, Queiro-Silva R, Martinez-Camblor P, Maldonado-Seral C, García-García B, Palacios-García L, Gomez-Bernal S, Santos-Juanes J, et al. Psoriasis, psoriatic arthritis and type 2 diabetes mellitus: a systematic review and meta-analysis. Br J Dermatol. 2013;169(4):783–793. doi:10.1111/bjd.12473.
46. Cheng J, Kuai D, Zhang L, Yang X, Qiu B. Psoriasis increased the risk of diabetes: a meta-analysis. Arch Dermatol Res. 2012;304(2):119–125. doi:10.1007/s00403-011-1200-6.
47. Wallrapp C, Hähnel S, Müller-Pillasch F, Burghardt B, Iwamura T, Ruthenbürger M, Lerch MM, Adler G, Gress TM. A novel transmembrane serine protease (TMPRSS3) overexpressed in pancreatic cancer. Cancer Res. 2000;60:2602–2606.
48. Fujiki Y, Hubbard AL, Fowler S, Lazarow PB. Isolation of intracellular membranes by means of sodium carbonate treatment: application to endoplasmic reticulum. J Cell Biol. 1982;93(1):97–102. doi:10.1083/jcb.93.1.97.
49. Bordier C. Phase separation of integral membrane proteins in Triton X-114 solution. J Biol Chem. 1981;256(4):1604–1607. doi:10.1016/S0021-9258(19)69848-0.
50. Wessel A, Flügge UI. A method for the quantitative recovery of protein in dilute solution in the presence of detergents and lipids. Anal Biochem. 1984;138(1):141–143. doi:10.1016/0003-2697(84)90782-6.
51. Tokuyasu KT, Maher PA. Immnocytochemical studies of cardiac myofibrillogenesis in early chick embryos. I. Presence of immunofluorescent titin spots in premyofibril stages. J Cell Biol. 1987;105(6):2781–2793. doi:10.1083/jcb.105.6.2781.